

Recent Experiments and Post-Discharge Modeling of the ElectricOIL Laser System

D. L. Carroll, J. T. Verdeyen, D. M. King, J. W. Zimmerman, J. K. Laystrom, A. D. Palla
CU Aerospace, 60 Hazelwood Dr., Champaign, IL 61820
B. S. Woodard, G. F. Benavides, K. Kittell, and W. C. Solomon
University of Illinois, 306 Talbot Laboratory, 104 S. Wright St., Urbana, IL 61801

ABSTRACT

In this paper we report on studies of a continuous wave laser at 1315 nm on the $I(^2P_{1/2}) \rightarrow I(^2P_{3/2})$ transition of atomic iodine where the $O_2(a^1\Delta)$ used to pump the iodine was produced by a radio frequency excited electric discharge. The electric discharge was sustained in He/ O_2 gas mixtures upstream of a supersonic cavity which is employed to lower the temperature of the continuous gas flow and shift the equilibrium of atomic iodine in favor of the $I(^2P_{1/2})$ state. The results of experimental studies for several different flow conditions and mirror sets are presented. The highest laser output power obtained in these experiments was 510 mW in a stable cavity composed of two 99.993% reflective mirrors. Blaze II laser model was used to model typical ElectricOIL conditions in the post-discharge region through the laser cavity. Overall the Blaze II simulation model appears to be predicting many of the observed qualitative trends that have been measured and the quantitative comparisons to data are reasonable.

Keywords: electric oxygen-iodine laser, ElectricOIL, RF excitation of oxygen, singlet-delta oxygen, DOIL

I. INTRODUCTION

The classic chemical oxygen-iodine laser (COIL) system¹ operates on the $I(^2P_{1/2}) \rightarrow I(^2P_{3/2})$ [hereafter denoted as I^* and I , respectively] electronic transition of the iodine atom at 1315 nm. The population inversion is produced by the near resonant energy transfer between the metastable excited singlet oxygen molecule, $O_2(a^1\Delta)$ [denoted $O_2(a)$ hereafter], and the iodine atom ground state $I(^2P_{3/2})$. Conventionally, the $O_2(a)$ is produced by a liquid chemistry generator with which there are many system issues having to do with weight, and safety that have motivated investigations into methods to produce $O_2(a)$ using flowing electric discharges. Early attempts to implement electric discharges to generate $O_2(a)$ and transfer to iodine to make a laser by Zalesskii² and Fournier³ did not result in gain. Over the past several years investigations into the possibility of a hybrid electrically powered oxygen-iodine laser have been performed with electric discharges to produce the $O_2(a)$.⁴⁻⁹ These studies have shown that flowing electric discharges through oxygen containing mixtures, typically diluted with a rare gas, can produce significant quantities of $O_2(a)$. Recent studies have demonstrated $O_2(a)$ yields greater than 15% using electric discharges,^{6,7,9} and modeling results^{4,7,8,10} indicated that such a system could produce a viable laser. Recently Carroll *et al.*^{11,12} reported direct measurements of positive gain in atomic iodine resulting from electric discharge produced $O_2(a)$ followed by a lasing demonstration¹³ in their Electric Oxygen Iodine Laser system (ElectricOIL). Following the measurement of positive gain in a supersonic flow,¹¹ Rawlins *et al.*¹⁴ measured positive gain in a higher temperature subsonic flow.

II. EXPERIMENTAL SETUP

A block diagram of the flow tube setup is shown in Fig. 1. A longitudinal radio frequency (rf) electric discharge at 13.56 MHz was used as the excitation source. This configuration will be discussed at more length in Section 4.1.

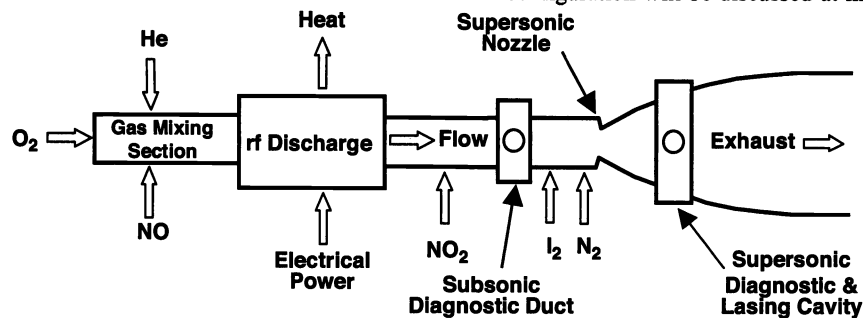


Figure 1: Schematic of experimental apparatus.

The supersonic diagnostic cavity has a Mach 2 nozzle with windows that serve as view ports. Upstream of the nozzle, the subsonic diagnostic duct has four windows through which simultaneous measurements are made of the optical emission from O₂(a) at 1268 nm, O₂(b¹Σ) [denoted O₂(b) hereafter] at 762 nm, I* at 1315 nm, and the gain/absorption proportional to [I*] – 0.5·[I]. A Roper Scientific Optical Multi-channel Analyzer (OMA-V) was used for measurements at 1268 nm and 1315 nm. A Santa Barbara Instruments Group, Inc. ST-6 CCD camera coupled to a Jarrell Ash M10023100 monochromator was implemented to measure the emission of O₂(b) at 762 nm.

Micro-Motion CMF and Omega FMA mass flow meters were used to measure the flow rates of the gases. The I₂ concentration was measured by a method developed by Physical Sciences Inc. (PSI) and is based on the continuum absorption of molecular iodine at 488 nm. Details of this diagnostic are described by Rawlins *et al.*¹⁵ Pressures in the subsonic and supersonic flow regions were measured by capacitance manometers. Incident and reflected powers from the rf matching network were measured by a Bird ThruLine model 43 wattmeter (rf “System Power” is the difference of the incident and reflected powers). Note that rf system power is presented in the plots; separate electrical measurements indicate that approximately 80-90% of the system power is actually absorbed by the plasma for the O₂:He=1:4 mixtures we ran in these experiments for the longitudinal discharge.

Measurements of gain (or absorption) were made using the Iodine-Scan Diagnostic (ISD) developed by PSI¹⁶ prior to installing the laser mirrors. The ISD is a diode laser based monitor for the small signal gain in iodine lasers. The system uses a single mode, tunable diode laser that is capable of accessing all six hyperfine components of the atomic iodine. It was calibrated in frequency to enable automated operation for the (3,4) hyperfine transition for our experiments. A fiber optic cable was used to deliver the diode laser probe beam to the iodine diagnostic regions in the subsonic portion of the flow tube and in the supersonic cavity. Since the ISD uses a narrow band diode laser, measurements of the lineshapes can also be used to determine the local temperature from the Voigt profile.

The windows on the sides of the cavity when using the gain diagnostic were wedged and anti-reflection coated to minimize etalon effects. A 2-pass configuration (10 cm path length) was used in the subsonic section and a 4-pass configuration (20 cm path length) was used in the supersonic section. Measurements of the O₂(a) yield {defined as $Y=O_2(a)/[O_2(X)+O_2(a)]$ } were obtained from the gain measurements, and the relative values of the spectral intensities measured for I* to O₂(a) using techniques originally developed by Hager,¹⁷ Davis and Rawlins.¹⁵ [Note that O₂(X) is used here as an abbreviation for the O₂(X³Σ) ground state of oxygen].

Laser power measurements were made with a Scientech Astral™ model AC2500/AC25H calorimeter interfaced to a Scientech Vector™ model S310 readout, and were made at the same location in the supersonic laser cavity as were the gain measurements. The gain measurements were made first. The vacuum mirror mounts were then installed for the laser power trials. Different sets of mirrors (discussed in Section III) formed a stable optical cavity. The mirrors were separated by 38 cm. An Infrared (IR) Detection Card from New Focus, Model 5842, with response between 800-1600 nm, was also used to observe the intensity profile of the beam.

III. MIRROR SELECTION AND MEASUREMENTS

The choice of mirror reflectivities was based on previous measurements of gain. For laser oscillations to occur, the gain coefficient at line center $\gamma_0(\nu_0)$ must satisfy

$$\gamma_0(\nu_0) \geq \frac{1}{2l_g} \ln\left(\frac{1}{R_1 R_2}\right) = \gamma_{th}(\nu_0) \quad (\text{threshold}) \quad (1)$$

where l_g is the length of the gain medium (5 cm for our experiment) and R_1 and R_2 are the mirror reflectivities. For similar flow conditions we previously¹² obtained a gain of $\approx 0.005\% \text{ cm}^{-1}$. With these values of gain and gain length, laser oscillation requires mirrors having reflectivity exceeding $R_1 R_2 = 0.99950$, or $R_1 = R_2 = 0.99975$. Based upon this requirement, mirrors were obtained having a reflectivity of $R > 0.9998$.

Table 1. Measurements of mirror transmissivity and estimated reflectivity from 1-T. Note that CC indicates a concave mirror.

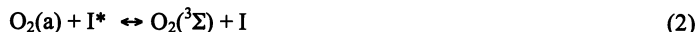
Mirror #	Curvature	Manufacturer	Transmissivity, T	Reflectivity, R
1	1m CC	LGR	0.000135	0.999865
2	1m CC	LGR	0.000143	0.999857
3	2m CC	LGR	0.000071	0.999929
4	2m CC	LGR	0.000070	0.999930

Different sets of mirrors with 1 m and 2 m radii of curvature were purchased from Los Gatos Research, Inc. (LGR). Table 1 lists measurements of the transmissivity, T, from which the reflectivity, R, was estimated as 1-T. The transmissivity was determined by using the ISD laser diode and measuring the signal from an InGaAs detector

coupled to a Stanford Research Systems Lock-in Amplifier Model SR530, with and without the mirror in the probe beam path. The probe beam signal for the transmission measurement was provided by the PSI gain diagnostic at 1315 nm. The transmission measurements were in close agreement with transmission curves provided by the manufacturers.

IV. EXPERIMENTAL RESULTS

Electric discharge stability and temperature were found to be critical parameters to obtaining gain.^{11,12} Electric discharges sustained in moderate pressures (5-15 of Torr) of oxygen are prone to arcing and constriction. The production of O atoms, O₃ and other excited species by the discharge adds higher levels of complexity (these species are not usually encountered in the purely chemical system) to the downstream kinetics when the iodine donor species are added to the flow. The critical aspect of temperature control results from the equilibrium of the pumping reaction,



where the forward rate is $7.8 \times 10^{-11} \text{ cm}^3/\text{molecule}\cdot\text{s}$,¹⁸ and the backward rate is $1.04 \times 10^{-10} \exp(-403/T) \text{ cm}^3/\text{molecule}\cdot\text{s}$.¹⁹ The equilibrium rate constant ratio of the forward to backward reactions is $K_{eq}=0.75 \exp(403/T)$,¹⁹ where T is the gas temperature. The yield of O₂(a) for optical transparency ($\gamma_{OT} = 0$), also known as the “threshold yield”, as a function of temperature is $Y_{OT}=1/[1+1.5 \exp(403/T)]$.²⁰ Note, the backward rate is slower, K_{eq} larger, and Y_{OT} lower as T is decreased.

4.1 Laser Performance with a Longitudinal rf Discharge

The first type of discharge implemented for these lasing studies was a radio frequency (rf) electric discharge at 13.56 MHz operated between two internal hollow cathode electrodes (each 10 cm long) oriented longitudinally in the same direction as the gas flow. For this longitudinal discharge, the plasma zone was approximately 4.9 cm in diameter and 25 cm long. Details of the performance of this electric discharge can be found in Carroll *et al.*⁵

Many flow conditions were investigated that resulted in gain and lasing using the configuration shown in Fig. 1. The experiments focused on a baseline case consisting of 3.0 mmol/s of O₂ mixed with 16.0 mmol/s of He running through the discharge. A tertiary flow of cold N₂ gas was injected further downstream to lower the temperature and to raise the pressure to improve the performance of the nozzle with our vacuum system. The discharge production of O₂(¹Δ) was enhanced by the addition of a small proportion of NO to lower the average ionization threshold and thereby also lower the sustaining value of E/N of the gas mixture,¹² therefore most experiments were run with NO in the discharge. In earlier experiments that achieved positive gain using slightly different flow conditions, NO₂ was used to scavenge excess O atoms,^{11,12} therefore some cases were run with NO₂ injected downstream of the discharge. The NO₂ injector ring was located 17.8 cm downstream from the exit of the longitudinal discharge. The I₂ injector ring was located 63.5 cm downstream from the exit of the longitudinal discharge. A tertiary N₂ diluent injector ring was located 78.7 cm downstream from the exit of the longitudinal discharge. Details of these experiments are provided in the following sections.

4.1.1 O₂/He/NO discharge experiments with NO₂ injected downstream

The initial lasing experiments were run with 3.0 mmol/s of O₂ mixed with 16.0 mmol/s of He and 0.15 mmol/s of NO flowing through the rf discharge. For these initial lasing tests, a flow rate of 0.23 mmol/s of NO₂ was used to scavenge excess O atoms. The NO₂ flow was accompanied by 2.0 mmol/s of carrier He diluent. The secondary stream consisted of ≈ 0.008 mmol/s of I₂ with 2.0 mmol/s of secondary He diluent. The tertiary flow was 38 mmol/s of cold N₂ gas at a temperature of ≈ 135 K. The pressures in the subsonic diagnostic duct and in the supersonic diagnostic cavity were 10.4 Torr and 1.35 Torr, respectively.

Gain for the above flow conditions at 450 W of rf discharge power is shown in Fig. 2 and peaks at 0.0067% cm⁻¹ at line center. The laser resonator was subsequently installed around the supersonic flow cavity and simultaneous measurements of O₂(a) yield and laser power were made using two 1 m concave mirrors with a reflectivity of ≈ 0.99986 , mirrors #1 and #2 from Table 1. For the above flow conditions and 450 W rf power, a laser output power of 178 mW was obtained. The yield of O₂(a) was $\approx 16\%$ with a temperature of ≈ 410 K in the subsonic diagnostic duct (upstream of the N₂ diluent injection) and a temperature in the supersonic cavity of ≈ 180 K from the lineshape measurement. The beam shape was circular with a diameter of ≈ 1.9 cm, the same as the clear aperture of the mirror mounts. For reference, the first measurement of laser action using a classic liquid chemistry COIL system produced 4 mW.¹

4.1.2 O₂/He/NO discharge experiments without NO₂ downstream

Three sets of experiments were run with the longitudinal rf discharge with NO in the discharge and without NO₂ downstream of the discharge. The conditions used in the first set of these experiments were 3.0 mmol/s of O₂ mixed with 16.0 mmol/s of He and 0.15 mmol/s of NO flowing through the rf discharge. The secondary stream consisting of ≈ 0.008 mmol/s of I₂ with 2.0 mmol/s of He diluent was injected 63.5 cm downstream from the exit of the discharge. A tertiary flow of 55 mmol/s of cold N₂ gas (≈ 120 K) was injected further downstream to lower the temperature and to raise the pressure to improve the supersonic nozzle performance. Using an NO₂ titration technique, the O atom flow rate at 500 W of rf power was measured to be approximately 0.13 mmol/s for these conditions with NO in the discharge (note that this titration technique is considerably more difficult with NO already running through the discharge). The pressures in the subsonic diagnostic duct and in the supersonic diagnostic cavity were 12.6 Torr and 1.55 Torr, respectively. For these conditions, no additional NO₂ was employed to scavenge excess O atoms; in fact, at this slightly higher pressure, adding NO₂ was deleterious to laser performance. The reason for this effect is not fully understood at the moment, but may be in part due to a lower O atom production or higher O atom loss rate at these higher pressure conditions.

Gain for the above flow conditions at slightly higher pressure and 450 W of rf discharge power is approximately the same as that from Section 4.1.1, shown in Fig. 2, and also peaks at 0.0067% cm⁻¹ at line center. The lineshape also indicates a temperature of ≈ 180 K. The laser resonator was subsequently installed around the supersonic flow cavity and simultaneous measurements of O₂(a) yield and laser power were made as a function of rf discharge power as shown in Fig. 3. For the above flow conditions and 450 W rf power, a laser output power of 207 mW was obtained. The yield of O₂(a) was $\approx 17\%$ with a temperature of ≈ 410 K in the subsonic diagnostic duct. (Note that the drop in O₂(a) signal beyond 400 W is believed to be a consequence of discharge instabilities such as thermal constriction that are visible in our discharge under these flow conditions¹²). The beam shape was also circular with a diameter of ≈ 1.9 cm, the same as the clear aperture of the mirror mounts.

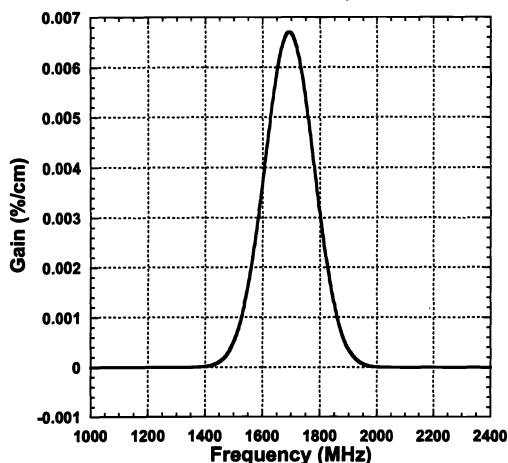


Figure 2. Digitally filtered gain signal in the supersonic cavity as a function of laser diode scan frequency measured prior to lasing experiments.

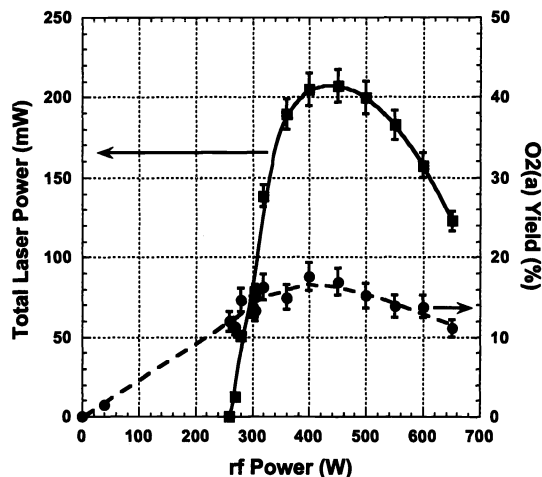


Figure 3. O₂(a) yield in the subsonic diagnostic section and total outcoupled laser power in the supersonic cavity as a function of rf discharge power. Subsonic flow tube pressure of 10 torr.

The threshold for laser oscillation lasing occurs at 260 W of rf discharge power and an estimated O₂(a) yield of 12% in the subsonic flow tube, as shown in Fig. 3. Note that there is a roll off in laser power beyond 450 W that is greater than the drop in O₂(a) yield which is in part attributed to discharge instabilities. Even in the absence of discharge instabilities, laser oscillation would likely decrease at higher powers for these conditions as a consequence of two factors: (i) higher powers result in higher gas temperatures and consequently lower gain and (ii) progressively more O atoms are generated at higher powers while the NO flow rate was optimized for 450 W. (An excess of O atoms have been found to quench the excited I* atom¹²). A long duration run time test was performed and the laser power was relatively stable at 220 mW \pm 10 mW for more than 33 minutes, as shown in Fig. 4. The cause of the small oscillations in Fig. 4 with a period of approximately 33 s corresponds to small fluctuations in the iodine source temperature (kept at 83°C \pm 2°C) and therefore is likely a consequence of small fluctuations in the iodine flow rate. A second long duration test was performed in which the rf power, and consequently the laser

power, was cycled on and off, Fig. 5; the power was found to be stable to within $\pm 2\%$ over a 32 minute test (the first 8 minutes are illustrated).

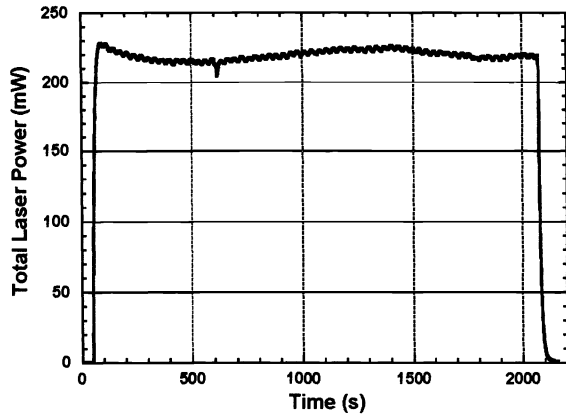


Figure 4. Continuous wave uncoupled laser power as a function of time

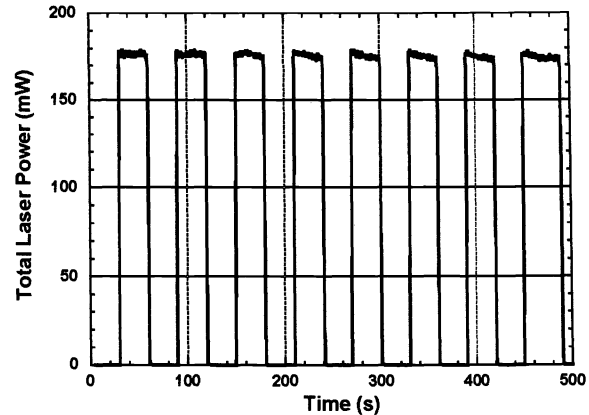


Figure 5. Continuous wave cycled laser power as a function of time.

A second series of experiments were run for three different mirror sets having different reflectivities. The same flow conditions discussed above were used for these experiments. Simultaneous measurements of laser power and $O_2(a)$ yield were made as a function of rf discharge power as shown in Fig. 6. For the above flow conditions a peak laser output power of 184 mW was obtained with the Mirror #1/#2 combination, 219 mW with the Mirror #1/#3 combination, and 234 mW with the Mirror #3/#4 combination. The yield of $O_2(a)$ was $\approx 17\%$ with a temperature of ≈ 410 K in the subsonic diagnostic duct for the peak power points. For all but the low laser output power points, the beam shape was circular with a diameter of ≈ 1.9 cm, the same as the clear aperture of the mirror mounts. The reasons for the drop in laser output power above 450 W of rf power are the same as discussed above for Fig. 3, i.e., discharge instabilities, higher temperature, and higher O atom production.

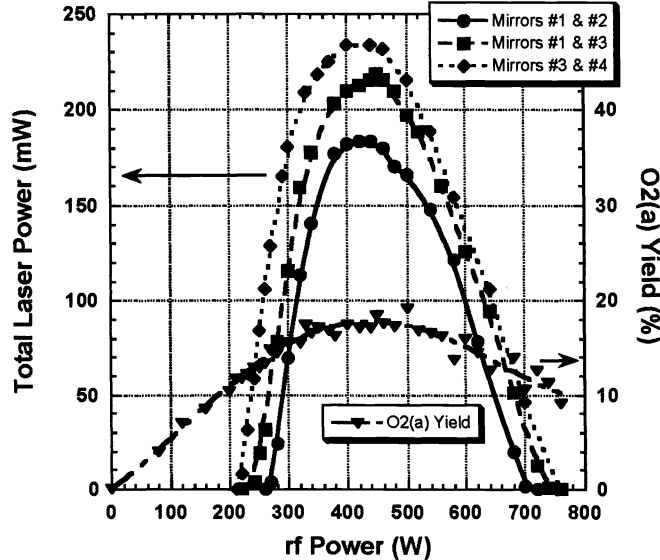


Figure 6. $O_2(a)$ yield in the subsonic diagnostic section and total laser power in the supersonic cavity as a function of rf discharge power, for three different mirror sets. Subsonic flow tube pressure of 12.5 torr.

There are several interesting points to make from Fig. 6. First, the laser output power was always higher with the progressively higher reflectivity mirrors. Along similar lines, the laser threshold shifted to lower rf power as the reflectivity of the mirrors increased; this is consistent with the required threshold gain γ_{th} being smaller for higher reflectance mirrors [from Table 1 and Eq. (1), $\gamma_{th}=2.8 \times 10^{-5} \text{ cm}^{-1}$ for the #1/2 mirror set, $\gamma_{th}=2.1 \times 10^{-5} \text{ cm}^{-1}$ for the #1/3 mirror set, and $\gamma_{th}=1.4 \times 10^{-5} \text{ cm}^{-1}$ for the #3/4 mirror set] and that the $O_2(a)$ yield and gain decrease with lower rf power. In other words, the data support the expectation that higher reflective mirrors will lase at a lower value of gain. Note also that there is a variation in peak output power for the data presented in Figs. 3-6 all having approximately the same flow conditions and the same #1/#2 mirror set; we believe that the differences are primarily

due to variations of a few degrees K in the day-to-day room temperature of the laboratory that consequently affected the vapor pressure of I₂ in the unheated I₂ sublimation cell.

4.1.3 O₂/He/NO discharge experiments without NO₂ injected downstream and varied I₂ flow

Post-discharge modeling of the experimental conditions discussed in Section 4.1.2 using the Blaze II kinetic/laser model²¹ indicated that increasing the I₂ flow rate should improve gain and laser power (Section 5). As such, experiments that varied the I₂ flow rate were performed. Other than the I₂ and the I₂ carrier gas (helium) flow rates, all of the other flow conditions were the same as discussed in Section 4.1.2. First, the secondary flow rate of helium was increased and was found to optimize laser power with a flow rate of 3.0 mmol/s of He rather than the 2.0 mmol/s used in Sections 4.1.1 and 4.1.2. The I₂ flow rate with a room temperature (25° C) I₂ sublimation cell temperature and 3.0 mmol/s of secondary He was 0.014 mmol/s of I₂. The laser power with the higher reflectivity #3 and #4 mirror set increased to 260 mW.

To obtain further increases in the iodine flow rate the iodine sublimation cell was heated. With a 3.0 mmol/s secondary flow rate of helium, the I₂ flow rate at ≈30° C was approximately 0.022 mmol/s, at ≈40° C the I₂ flow rate was approximately 0.036 mmol/s, and at ≈50° C the I₂ flow rate was approximately 0.052 mmol/s. The power optimized around an I₂ flow rate of 0.040 mmol/s. Small signal gain and laser power measurements were made for the I₂ flow rates of 0.022 and 0.036 mmol/s as a function of rf power, Figs. 7 and 8. The laser measurements were made using the #3/#4 mirror set.

Figure 7 shows that the gain increased substantially with the higher iodine flow rate, going from a peak of approximately 0.0077% cm⁻¹ to 0.0156% cm⁻¹, roughly a factor of two increase in gain. This result is consistent with the significantly higher laser power that was measured for the 0.036 mmol/s of I₂ case, Fig. 8. The total laser power that was measured for the 0.036 mmol/s of I₂ case was 440 mW. A few additional measurements produced as high a power as 510 mW for a slightly higher I₂ flow rate of 0.040 mmol/s. The lineshapes from the gain profiles (not illustrated for brevity) indicated laser cavity temperatures of ≈160 K for the 0.022 mmol/s I₂ case and ≈190 K for the 0.036 mmol/s I₂ case. Note that a higher I₂ flow rate should result in more heat release from chemical reactions, consistent with the lineshapes that indicated a higher temperature with more I₂ flow.

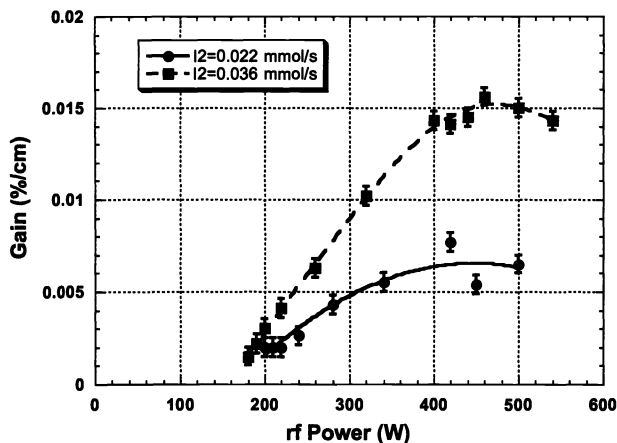


Figure 7. Gain in the supersonic cavity as a function of rf discharge power, for two different iodine flow rates. Subsonic flow tube pressure of 12.5 torr.

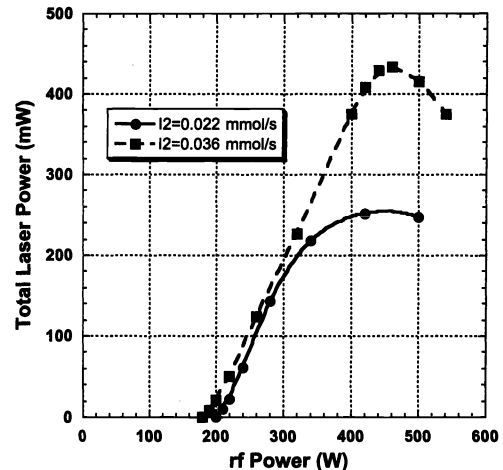


Figure 8. Total outcoupled laser power in the supersonic cavity as a function of rf discharge power, for two different iodine flow rates. Subsonic flow tube pressure of 12.5 torr.

4.1.4 O₂/He discharge experiments without NO and with NO₂ injected downstream

Because NO was found to enhance the production of O₂(a) by approximately 30-50% when run through the discharge,¹² a very limited number of experiments were performed without NO in the discharge. Using an NO₂ titration technique, the O atom flow rate at 500 W of rf power was measured to be approximately 0.33 mmol/s for these conditions without NO in the discharge. Using the #3 and #4 mirror combination, a total of 132 mW of outcoupled laser power was measured with zero NO flow and an NO₂ flow rate of 0.35 mmol/s. The I₂ flow rate was approximately 0.027 mmol/s. Other than the NO, NO₂, and I₂ flow rates, all of the other flow conditions were the same as discussed in Section 4.1.2. Note that when zero NO and zero NO₂ were used that we were unable to

obtain lasing. While lasing was demonstrated without NO in the discharge and with NO₂ added downstream to remove excess atomic oxygen, the performance was worse without NO in the discharge in all cases.

V. POST-DISCHARGE MODELING

For the post-discharge and laser system modeling we utilize the Blaze II laser simulation code,²¹ which contains one-dimensional fluid dynamic equations whose mixing terms were derived from the two-dimensional equations that describe the mixing flowfield in a gas laser cavity. The Blaze model can be used for mixing or premixed, axisymmetric and two-dimensional flows and has proven to be a robust and useful modeling tool for over 25 years for several different types of gas and chemical lasers. The use of the Blaze model for ElectricOIL simulations is discussed at length by Carroll *et al.*⁴ The Blaze II kinetic and laser model was implemented to better understand the kinetic phenomena that are being observed experimentally in the post-discharge and laser cavity portions of the experimental apparatus. Blaze II was also used to make preliminary power estimates for typical ElectricOIL conditions discussed in Section 4. The post-discharge and laser cavity chemistry is described in Ref. 4, with the exception of reaction (3), which has since been found to be critically significant.¹² Based upon work in Ref. 12 the Blaze modeling presented here includes reaction (3) with a rate of 3.5×10^{-12} cm³/molecule-s.



The Blaze simulations start from the exit of the discharge and proceed downstream through the flow tube and laser cavity. There are two additional injection points after the discharge: I₂/He was injected 81.9 cm and cold N₂ at 117.5 cm downstream from the discharge exit; the nozzle throat is located at 141.6 cm. All of the simulations discussed in this paper are premixed calculations where the injected flows are discontinuously added at the injection location and the computation is then continued as fully mixed. For the flow conditions discussed in Section 4.1.2 with an rf power of 450 W, the predicted O₂(a) yield as a function of distance from the discharge exit is shown in Fig. 9 for three different I₂ flow rates. There are four interesting features that are observed in Fig. 9:

- (i) the initial drop in O₂(a) yield is principally due to the O₂(a)+O₂(a) → O₂(b)+O₂ pooling reaction and a three body quenching reaction O₂(a)+O₂+O → O₂+O₂+O suggested in Ref. 9 that was included in our modeling;
- (ii) higher I₂ flow rate results in lower O₂(a) yields downstream in the laser cavity, which is in large part due to the effects of the I*+O quenching reaction (3);
- (iii) the rise in yield after the cold N₂ injection occurs from the O₂(b)+N₂ → O₂(a)+N₂ deactivation channel,²² where new O₂(b) has been created via O₂(a)+I* → O₂(b)+I after the iodine injection position;
- (iv) the yield after the nozzle throat drops as the pumping reaction (2) shifts in favor of I* as the temperature drops in the supersonic expansion.

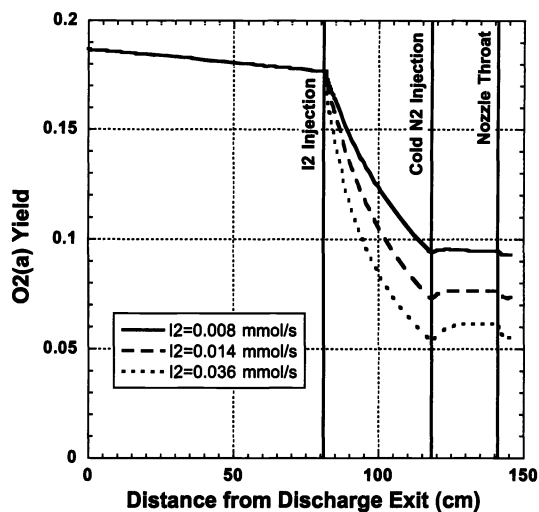


Figure 9. Blaze II predictions of O₂(a) yield vs. distance from the discharge exit as a function of I₂ flow rate.

Figures 10 and 11 illustrate the predicted gain for these three I₂ flow rates. A large drop in gain (increase in absorption) is observed between the I₂ injection location and the N₂ injection location, which is due to the I*+O quenching that ultimately reduces both the I* and O₂(a) concentrations. There is a sudden rise in gain when the cold N₂ is injected, which is a consequence of the pumping reaction (2) favoring colder temperatures; note that the gain then lowers as heat is transferred from the warmer wall to the cooler flow between N₂ injection position and the

nozzle throat (Blaze II includes a first order wall heat transfer term). Downstream of the throat the gain increases significantly in the supersonic cavity, Fig. 11. For I_2 flow rates of 0.008, 0.014, and 0.036 mmol/s the peak gain in the nozzle is predicted to be approximately 0.0080 %/cm, 0.0106 %/cm, and 0.0158 %/cm, respectively. As shown in Fig. 11, the prediction of gain for both the 0.008 mmol/s of I_2 and the 0.036 mmol/s of I_2 cases are in reasonably good agreement with the measured gains of 0.0067 %/cm (from Fig. 2) and 0.015 %/cm (from Fig. 7), respectively, for these conditions.

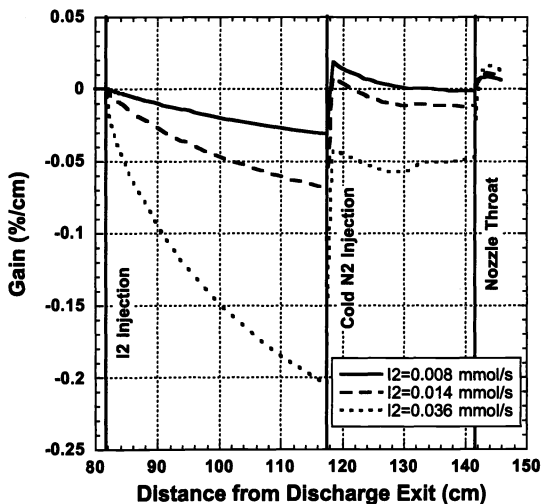


Figure 10. Blaze II predictions of gain vs. distance from the discharge exit as a function of I_2 flow rate.

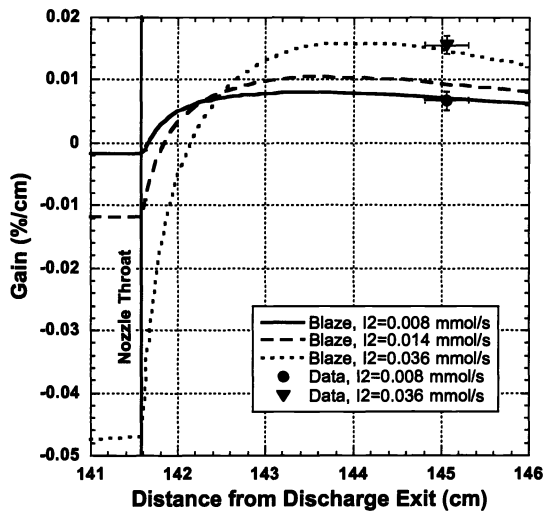


Figure 11. Blaze II predictions of gain vs. distance from the discharge exit (zoomed in to nozzle cavity region) as a function of I_2 flow rate.

Power predictions from Blaze are compared with measured data in Fig. 12 (the data are the peak powers from Fig. 6). Clearly Blaze is over-predicting the power. The Blaze calculation assumes mirrors that are the size of the flow channel, however, the experiments used 1" diameter optics with a 0.75" diameter opening that is smaller than the physical flow channel at the lasing position. As such, the Blaze calculations were adjusted lower to account for lasing in only a portion of the flow channel, however the simulation still over predicts the measured power. We are presently uncertain as to why the gain is being predicted with reasonable accuracy, yet the power is not; we are investigating this issue.

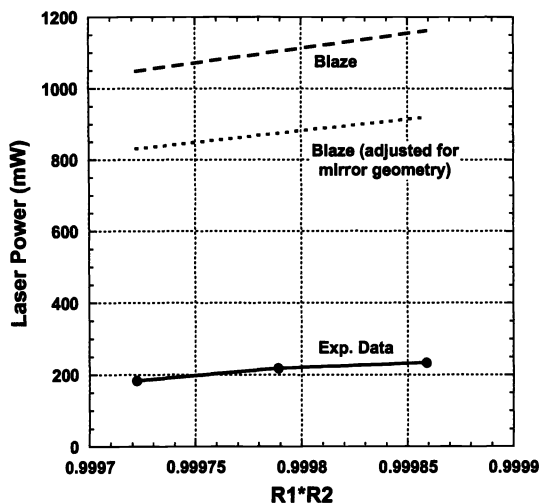


Figure 12. Blaze II predictions of laser power compared with experimental data as a function of the product of the mirror reflectivities.

VI. CONCLUDING REMARKS

In conclusion, cw laser action was measured on the $I^* \rightarrow I$ electronic transition of the iodine atom at 1315 nm pumped by a near resonant energy transfer from $O_2(a)$ produced in an electric discharge. A tertiary cold gas injection followed by expansion in a supersonic cavity was employed to lower the temperature of the flow and shift the equilibrium of atomic iodine in favor of the I^* state. This produced sufficient population inversion to observe gains of as high as $\approx 0.015\% \text{ cm}^{-1}$. Laser oscillations were obtained for differing flow conditions when two high reflectivity mirrors were used to form an optical resonator surrounding the gain medium. Lasing was achieved under a variety of flow conditions with a longitudinal rf discharge:

1. An $O_2/He/NO$ mixture running through the discharge and with NO_2 added downstream to remove excess atomic oxygen;
2. An O_2/He mixture running through the discharge with NO_2 added downstream to remove excess atomic oxygen;
3. An $O_2/He/NO$ mixture running through the discharge in the absence of NO_2 added downstream;
4. An $O_2/He/NO_2$ mixture running through the discharge in the absence of NO_2 added downstream.

The highest laser output power obtained in these experiments was approximately 510 mW in a stable cavity composed of two $\approx 99.993\%$ reflective mirrors. One set of experiments demonstrated a laser output power of 220 mW that was stable for more than 30 minutes, and another set of experiments demonstrated the ability to cycle the electrical power on and off to produce repeatable laser power over a 30 minute period.

Overall the Blaze II simulation model appears to be predicting many of the observed qualitative trends that have been measured, and the quantitative comparisons to gain data are quite reasonable. However, it is clear that improvements can be made with the modeling. We believe one factor that will add significantly to the accuracy of the predictions is to perform mixing simulations rather than the premixed calculations that were run in this study. Improvements in the accuracy of the kinetics will likely also play a crucial role in improved modeling of the system.

ACKNOWLEDGEMENTS

This work was supported by the Air Force Office of Scientific Research (AFOSR) and the Missile Defense Agency (MDA) through the U.S. Army Space and Missile Defense Command (USA/SMDC). The authors would like to acknowledge the contributions of: T. Madden and G. Hager (Air Force Research Laboratory); M. Kushner and D.S. Stafford (University of Illinois at Urbana-Champaign); S. Davis, T. Rawlins and B. Kessler (PSI, Inc.); M. Heaven and K. Morokuma (Emory University); G. Perram (Air Force Institute of Technology); M. Berman (AFOSR); J. Mulroy (MDA); B. Otey (USA/SMDC); D. Baer (Los Gatos Research); A. Ionin (P.N. Lebedev Physics Institute); A. Napartovich (Troitsk Institute for Innovation and Fusion Research); and T. Rakhimova (Lomonosov Moscow State University). We would also like to thank T. Field for his technical assistance.

REFERENCES

1. W. McDermott, N. Pchelkin, D. Benard, and R. Bousek, *Appl. Phys. Lett.* **32** (8) 469 (1978).
2. Zalesskii, V. Yu., *Zh. Eksp. Teor. Fiz.*, **67** 30 (1974) [*Sov. Phys. JETP* **40** (1) 14 (1975)].
3. G. Fournier, J. Bonnet, and D. Pigache, *J. Physique* **41** Colloque C9, 449 (1980).
4. D.L. Carroll, J.T. Verdeyen, D.M. King, B.S. Woodard, L.W. Skorski, J.W. Zimmerman, and W.C. Solomon, *IEEE J. Quant. Elect.* **39** (9) 1150 (2003).
5. D.L. Carroll, J.T. Verdeyen, D.M. King, B.S. Woodard, J.W. Zimmerman, L.W. Skorski, and W.C. Solomon, "Recent Experimental Measurements of the ElectricCOIL System," AIAA Paper 2003-4029 (2003).
6. J. Schmiedberger, S. Hirahara, Y. Ichinoche, M. Suzuki, W. Masuda, Y. Kihara, E. Yoshitani, and H. Fujii, *SPIE Vol. 4184* 32 (2001).
7. A.E. Hill, in *Proc. of the International Conf. on Lasers 2000*, ed. by V. Corcoran and T. Corcoran (STS Press, McClean, VA, 2001) 249.
8. A.A. Ionin, Y.M. Klimachev, A.A. Kotkov, I.V. Kochetov, A.P. Napartovich, L.V. Seleznev, D.V. Sinitsyn, and G.D. Hager, *J. Phys. D: Appl. Phys.* **36** 982 (2003).
9. T.V. Rakhimova, A.S. Kovalev, A.T. Rakhimov, K.S. Klopovsky, D.V. Lopaev, Y.A. Mankelevich, O.V. Proshina, O.V. Braginsky, and A.N. Vasilieva, "Radio-Frequency Plasma Generation of Singlet ($a^1\Delta_g$) Oxygen in O_2 and $O_2:Ar$ (He) Mixtures," AIAA Paper 2003-4306 (2003).
10. D.S. Stafford and M.J. Kushner, *J. of Appl. Phys.* **96** (5) 2451 (2004).
11. D.L. Carroll, J.T. Verdeyen, D.M. King, J.W. Zimmerman, J.K. Laystrom, B.S. Woodard, N. Richardson, K. Kittell, M.J. Kushner and W.C. Solomon, *Appl. Phys. Lett.* **85** (8) 1320 (2004).

12. D.L. Carroll, J.T. Verdeyen, D.M. King, J.W. Zimmerman, J.K. Laystrom, B.S. Woodard, G.F. Benavides, K. Kittell, and W.C. Solomon, *IEEE J. Quant. Elect.* **41** (2) 213 (2005).
13. D.L. Carroll, J.T. Verdeyen, D.M. King, J.W. Zimmerman, J.K. Laystrom, B.S. Woodard, G.F. Benavides, K. Kittell, D.S. Stafford, M.J. Kushner and W.C. Solomon, *Appl. Phys. Lett.* **86** 111104 (2005).
14. W.T. Rawlins, S. Lee, W.J. Kessler, and S.J. Davis, *Appl. Phys. Lett.* **86** 051105 (2005).
15. W.T. Rawlins, S.J. Davis, S. Lee, M.L. Silva, W.J. Kessler, and L.G. Piper, "Optical Diagnostics and Kinetics of Discharge-Initiated Oxygen-Iodine Energy Transfer," AIAA Paper 2003-4032 (2003).
16. S.J. Davis, M.G. Allen, W.J. Kessler, K.R. McManus, M.F. Miller, and P. Mulhall, *SPIE* Vol. **2702**, 195 (1996).
17. G.D. Hager (private communication).
18. R.G. Derwent and B.A. Thrush, *Discuss. Faraday Soc.*, **53**, 162 (1972).
19. G.P. Perram and G.D. Hager, "The Standard COIL Kinetics Package," Air Force Weapons Laboratory, Kirtland Air Force Base, Final Report AFWL-TR-88-50 (1988).
20. J. Hon, G. Hager, C. Helms, and K. Truesdell, *AIAA Journal*, **34**, 8, 1595 (1996).
21. L. Sentman, M. Subbiah, and S. Zelazny, "Blaze II: A Chemical Laser Simulation Computer Program," Bell Aerospace Textron, Buffalo, NY, T.R. H-CR-77-8 (1977).
22. R. Atkinson, D.L. Baulch, R.A. Cox, R.F. Hampson, Jr., J.A. Kerr, M.J. Rossi, and J. Troe., *J. Phys. Chem. Ref. Data*, **26**, 3, 550-962 (1997).